

Selection of Acquisition Channels of a Low-Cost Electroencephalogram Device for Signals Based on Motor Imagery for BCI using Typical Testors

Paula Rodríguez-Azar, María Dolores Torres Soto, Aurora Torres Soto, José Manuel Mejía Muñoz, and Carlos Alberto Ochoa

Abstract—Brain-computer interfaces based on motor imagination use the intention of movement to communicate with some external device, generally, the signals are acquired, processed, classified, and converted into control commands. However, one of the challenges to establishing interfaces in real-time is the reduction of the dimension of the data, since this increases the delay that exists between the intention of movement and the execution of the action in the device to be controlled. To reduce the delay, this study presents an analysis using typical testors, which are a tool that helps to find patterns in the electroencephalographic signals of motor imagination and thus helps to select the acquisition channels that provide the greatest amount of information. A subject participated in the study, from whom signals of two motor imagination thoughts were acquired, after the analysis of testors, the signals were classified with a recurrent neural network, and the result obtained was 97% accuracy.

Index Terms—Brain-computer interface (BCI), typical testors, electroencephalogram, motor imagery, LSTM.

I. INTRODUCTION

Brain-computer interfaces (BCI) use brain signals to communicate with an external device, which can be focused on neurorehabilitation and control. A BCI system involves the stage of signal acquisition, processing, and classification and finally, an application is assigned, Figure 1 shows this process. Recent studies have focused on the development of BCIs to help people with motor disabilities and improve their quality of life [1].

BCIs are classified into invasive and noninvasive systems according to the technique of brain information acquisition. One of the most commonly used noninvasive techniques is electroencephalography (EEG). Electroencephalography records the electrical activity generated by billions of brain neurons; the signals are recorded as temporal waves [2].

These signals can be classified according to the location of the acquisition channel, according to the international 10-20 system, morphology, amplitude, and frequency. The latter is studied through frequency bands which are delta (0.5 to 4Hz), theta (4 to 7Hz), alpha (8 to 12 Hz), and beta (13 to 30 Hz) [4].

Brain signals can be evoked or induced, the former is generated by external stimuli, the latter by the individual's intention to move. Recent studies have reported the technique

of motor imagination (MI), MI is an induced mental process, which consists of imagining some physical movement of a limb; through this process, sensorimotor modulations (SMR) are generated, which are divided into event-related synchronization (ERS) and event-related desynchronization (ERD), through ERS/ERD the signal is attenuated and generates an intention which is translated into control commands within the BCI's [5].

Currently, there are electroencephalogram devices with dry electrodes; these devices are portable and easy to place, which has benefited the development of brain-computer interfaces.

For BCI development, is important to acquire information from the different regions of the cerebral cortex, therefore devices with the largest number of sensors are generally sought, however, the robustness of the processing and classification algorithm is inversely proportional to the amount of information. Thus, reducing the dimensionality of the data is important, mainly for real-time BCI performance.

Therefore, this research has two main objectives which are:

- 1) Decrease the dimensionality of the data for future implementation in a real-time BCI.
- 2) Find which sensors and brain regions provide the most information to the BCI through MI thinking.

To this end, in this research we propose to perform an analysis of the EEG channels of the low-cost OpenBCI device that has eight sensors, using the method of typical testers, which is a method of combinatorial logic that enables eliminating identify the channels that give us more information in the classification of the data, this information is important because with it we can make decisions about the number of minimum sensors needed to reduce the dimensionality of the data, also allows us to identify the most active brain regions in the MI. Subsequently, we propose to classify the signals with a recurrent neural network model using the data obtained through the typical testers, for this experiment we used EEG signals from two types of thoughts of a subject.

The main contribution to the state of the art with this experiment is to demonstrate that the typical testor method can help to optimize brain-computer interfaces through the selection of the acquisition channels of a low-cost device.

Section two presents the work related to the selection of EEG signal acquisition channels, discusses typical testors, and explains LSTM neural networks, section three shows the

Manuscript received 18/01/2021, accepted for publication on 13/06/2021.

P. Rodríguez-Azar, J.M. Mejía Muñoz and C.A. Ochoa are with the Universidad Autónoma de Ciudad Juárez, Instituto de Ingeniería y Tecnología, Doctorado en Tecnología, Ciudad Juárez, Chihuahua, Mexico (jose.mejia@uacj.mx).

M. Dolores Torres Soto, A. Torres Soto are with the Universidad Autónoma de Aguascalientes, Doctorado en Ciencias Aplicadas y Tecnologías (DCAT), Aguascalientes, Aguascalientes, Mexico.

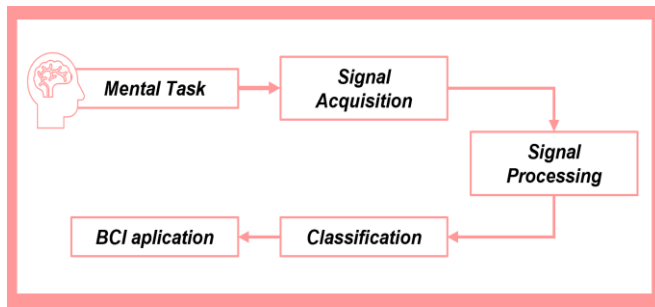


Fig. 1. Process of a brain-computer interface, which includes performing the mental task, acquiring the signals, processing and classifying the signals, and finally giving it an application [3]

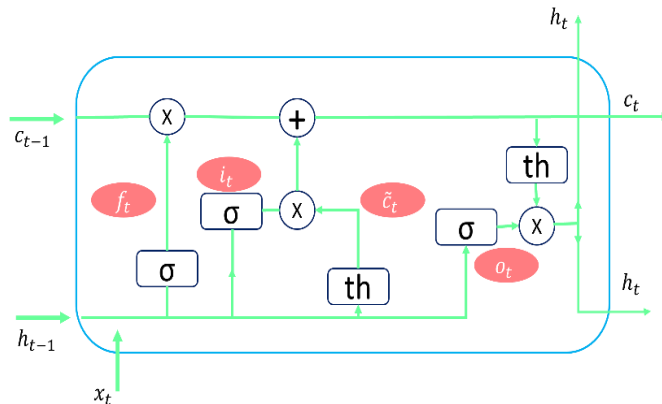


Fig. 2. LSTM recurrent neural network [18]

methods and materials used in the experiment, section four shows the results, and finally, section five discusses conclusions and future work.

II. BACKGROUND

MI signals are widely used in the development of BCIs, efficient selection of acquisition channels would help to optimize BCI interfaces. Recent studies have focused on the analysis of EEG channel selection for data dimensionality reduction of MI signals. Baig et. al [6] classify channel selection algorithms into three main types: filtering techniques, wrapper methods, and hybrid methods. In filtering techniques, we find correlation criteria such as Pearson's coefficient, mutual information, and algorithms such as Chi-square, as well as statistical techniques based on location, variance, redundancy, and relevance. Wrapper techniques use the objective function to evaluate the subset, usually using sequential selection algorithms and heuristic search algorithms. Hybrid techniques use a combination of filtering and wrapping techniques to obtain the advantages of both, that is, the accuracy of filtering and the adaptability of wrapping techniques.

Within the above classification studies such as that of Gaur et al. [7] who achieved a 65% reduction of acquisition channels by common spatial pattern (CSP). Liu et al. [8] used the genetic algorithm to find combinations of EEG channels and maximize classification accuracy. In [9], the selection of EEG channels is performed using hybrid optimization techniques based on the binary flower-pollination algorithm (FPA) and beta hill climbing. Hussien et al. [10] propose the modified gray wolf optimization algorithm for channel selection from the BCI Competition IV database.

On the other hand, in the study by Park and Chung [11], who used common spatial patterns (CSP) for channel selection in conjunction with the Fisher score, in this study the BCI competition III dataset 2a database was used, and an average accuracy of 88.62% was obtained.

In addition, channel selection techniques considered embedded techniques have also been proposed, such as the case of Zhang et al. [12], who proposed an approach based on deep learning, they used the squeeze-and-excitation module for channel selection, in addition to a convolutional neural network for the classification of left and right-handed MI, they obtained an average accuracy of 87%. Furthermore, the study of Jin et al. [13], used bispectrum analysis for nonlinear and non-Gaussian signals for the classification of tree databases, including BCI competition IV dataset 1, in which they obtained an accuracy of 83%.

Another interesting study is by Varsehi and Firoozabadi [14], where they used Granger causality (GC) in conjunction with a machine learning approach for the physionet MI database, resulting in an accuracy of 93%. One of the best results found in the literature was the study by Gurve et. al [15] who used non-negative matrix factorization, in addition to neighborhood component analysis for the selection of subject-specific characteristics, where they analyzed 10 healthy subjects and obtained an accuracy of 96%.

Our method is based on pattern recognition, which is a technique that takes characteristics directly from the data independently of the classifier. In the following, we will explain the typical testor method and the classification algorithm.

A. Typical Testor

A typical testor is a concept belonging to the combinatorial logic approach within pattern recognition. The typical testor is the minimum set of features that allows to discriminate of objects belonging to different classes, these are searched among all possible subsets of columns of features [16,17].

Let U be a set of objects of N characteristics grouped into C classes. By comparing the features of each object with those of objects belonging to different class in the form of pairs, we obtain the difference matrix $DM = [m_{ij}] [m_{ij}]_{L \times N}$ where $m_{ij} \in \{0, 1\}$ and L is the number of pairs, i the number of objects, j the feature. For $m_{ij} = 1$ the stated equality criterion is not satisfied, whereas for $m_{ij} = 0$ the equality criterion is satisfied for j .

Considering that $I = \{i_1, \dots, i_j\}$ is the set of rows, $J = \{j_1, \dots, j_n\}$ the set of features.

$T \subseteq J$ where T is a DM testor if they meet the following definitions:

1. a set $T = \{j_{k1}, \dots, j_{kl}\} \subseteq J$ is an DM testor if there is no row of zeros.
2. The characteristic $j_{kr} \in T$ is typical with respect to T and DM if $\exists q$, where $q \in \{1, \dots, L\}$ such that $a_{i_q j_{kr}} = 1$ for $S > a_{i_q j_{kp}} = 0 \forall p \text{ for } p \in \{1, \dots, S\} p \neq r$.
3. A set T has the typicality property with respect to a basic matrix BM if all the characteristics in T are typical with respect to T and DM .

Only if an identity matrix can be obtained in the testor matrix TM , by eliminating and interchanging some rows.

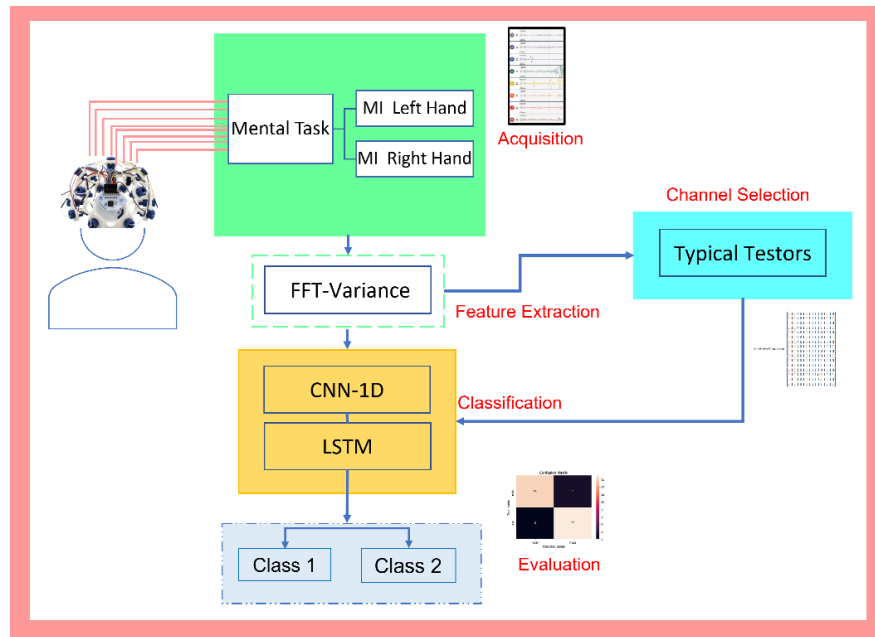


Fig. 3. Methodology used to determine the acquisition channels that provide the most information for the classification of brain signals

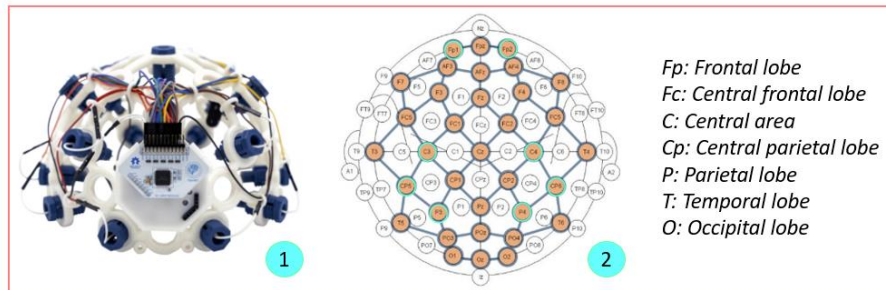


Fig. 4. OpenBCI device, 1: Physical dry sensor device. 2: device configuration for the acquisition of EEG signals [19]

B. LSTM

Recurrent neural networks (RRN), are neural networks designed to process sequential data, one of the most used neural networks in recent studies is the long short-term memory (LSTM). The LSTM processes sequential data through gates, uses the input signal and converts it into four variables, which pass through three gates and a hyperbolic tangent. Figure 2 shows the LSTM diagram.

The output of the network depends on the data input and, in turn, on the weights and parameters of the previous output during model training [18]. The LSTM is given by equations 1,2,3,4,5:

$$f_t = \sigma(W_{xf}x_t + W_{hf}h_{t-1} + W_{cf}c_{t-1} + b_f), \tag{1}$$

$$i_t = \sigma(W_{xi}x_t + W_{hi}h_{t-1} + W_{ci}c_{t-1} + b_i), \tag{2}$$

$$c_t = f_t c_{t-1} + i_t \tanh(W_{xc}x_t + W_{hc}h_{t-1} + b_c), \tag{3}$$

$$o_t = \sigma(W_{xo}x_t + W_{ho}h_{t-1} + W_{co}c_t + b_o), \tag{4}$$

$$h_t = o_t \tanh(c_t), \tag{5}$$

where σ is the sigmoid logistic function, W_t is the weight obtained during training x_t is the input, f_t is the forgetting gate, i_t is the input gate, c_t is the update cell, o_t is the output gate, and h_t is the output.

III. METHODS AND MATERIALS

The methodology and materials used in the experiment are shown below, the brain signals were acquired, and processed, using the testors technique the channels that provide the most relevant information were determined, and finally using the channels of the testors result were classified with RRN. Figure 3 shows the methodology used.

A. Electroencephalogram Signal Acquisition

One 30-year-old subject participated in this study, who are right-handed, sleep between 6 and 8 hours a day, consume a cup of coffee a day, exercise 3 to 5 days a week, do not smoke, do not consume alcohol, and have no diagnosed mental illness or neurological disorder.

A low-cost EEG device called OpenBCI with the Cython acquisition card with 250Hz sampling rate was used for acquisition. The device is shown in Figure 4, it has 8 acquisition channels, which are composed of dry electrodes. Channels FP1, FP2, C3, C4, CP5, CP8, P3, P4 were used for this experiment, according to the international electrode placement system 10 20.

The signals were acquired with ambient lighting conditions between 100 and 200 luxes, noise between 30 and 40 decibels,

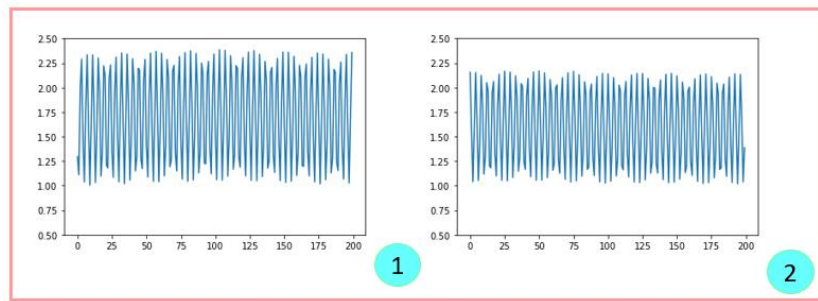


Fig. 5. Plot of the signals from the same recording. 1: MI right-hand thought signal. 2: Left hand MI thought signal

temperature between 18 and 26 degrees Celsius and ventilation generated by air conditioning units.

A total of 30 recordings were made during two sessions. At the beginning, the subject was requested to relax for 5 minutes to lower the heart rate. The mental tasks were the imagination of the movement of opening and closing the left hand (left hand MI), imagination of the movement of opening and closing the right hand (right hand MI). The acquisition time per recording was 1 minute 40 seconds of which 80 seconds are to perform the mental tasks and the remaining 20 seconds are due to the duration of the audio of the interface created to give instructions to the subject for each mental activity.

Before starting, the subject was instructed to sit in a comfortable position with arms relaxed and hands on the quadriceps, and was asked to close his eyes and avoid blinking. During the acquisition, the first 10 seconds of preparation were used where the subject prepares mentally and physically to perform the metal tasks, followed by 10 seconds of MI right hand, 10 seconds rest in which the subject stops thinking about something specific, 10 seconds of MI left hand, 10 seconds rest, 10 seconds of MI right hand, 10 seconds rest and finally 10 seconds of MI left hand.

B. Preprocessing

During preprocessing, the signals were converted from .txt files to .csv files. These signals were segmented into arrays of [2000,8] per class, which is equivalent to 8 seconds per task from which 60 signals per class were obtained, a total of 120. Figure 5 shows a printout of a right-hand MI and left-hand MI signal taken during the same recording.

C. Processing

Once the segments were obtained for each mental task, the signals were transferred from the time domain to the frequency domain using the Fast Fourier Transform (FFT), which is an implementation of the Discrete Fourier Transform (DFT) and in our case converts the signals into N components from 0 to 250HZ using equation 6, where x_n is the periodic signal:

$$x_k = \sum_{n=0}^{N-1} x_n e^{(-\frac{2\pi}{N})kn}, k = 0, \dots, N - 1. \tag{6}$$

Subsequently, the variance of the FFT components was calculated. For which an array of dimensions [8,120] was obtained, that is 120 signals and one feature per channel for each class.

Once the signal characteristics were obtained, in order to manipulate and compare the characteristics more easily the data were discretized, at this stage, the data were sorted and divided into ten segments using the classical K-means algorithm, this method consists of grouping the data set into k subsets from its mean value.

D. Channel Selection Using the Typical Testor Method

From the discretized matrix, the learning matrix *LM* of 120 rows and 8 columns is established, which belong to the signals and characteristics per channel respectively, the objects of class 1 (left hand MI) are compared with respect to class 2 (right hand MI) using the strict equality criterion, where 0 represents equality and 1 represents the difference between each comparison. From this, an *DM* of 3,136 rows and 8 columns was obtained. Subsequently, all redundancy was eliminated, obtaining the *BM* of testors of dimension [3,8] in array 7 the *BM* is shown:

$$BM = \begin{matrix} 0 & 0 & 0 & 0 & 0 & 1 & 0 \\ 0 & 0 & 1 & 0 & 0 & 0 & 0 \\ 1 & 1 & 0 & 0 & 0 & 0 & 1 \end{matrix} \tag{7}$$

On the other hand, the power set *PS* is generated, which shows all the subsets of the two classes $C = \{0, 1\}$, raised to the power *N*, where 0 is the left-hand MI class, 1 is the right-hand MI class and *N* is the number of characteristics as seen in equation 8:

$$PS = C^N = 2^8 = 256 \times 8. \tag{8}$$

The *BM* is multiplied by *PS* generating an array of typical testors from [56, 8]. Finally reducing all redundancy, we obtained a single typical testor which is observed in array 9:

$$Typical\ testor = \begin{matrix} C1 & C2 & C3 & C4 & C5 & C6 & C7 & C8 \\ 0 & 0 & 1 & 0 & 0 & 0 & 1 & 1 \end{matrix} \tag{9}$$

E. Classification of the Selected Channels with the Typical Testor Method.

A hybrid neural network CNN-1D and LSTM with 70 neurons was used for the classification, the model can be seen in Figure 6. The training was performed using the data containing the variance characteristics of the FFT, for which the most relevant channels resulting from the typical tester were used. These channels are channel 3, channel 7 and channel 8, which correspond to channel C3, C7 and C8.

The data set was divided for training and validation, 70% of the data was used for training, the remaining 30% was used only

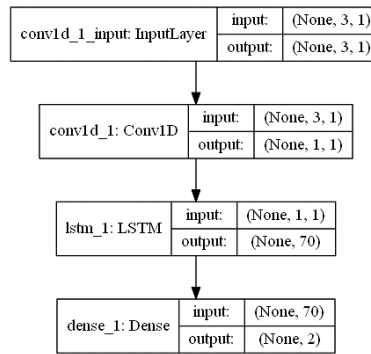


Fig. 6. Model of the recurrent neural network

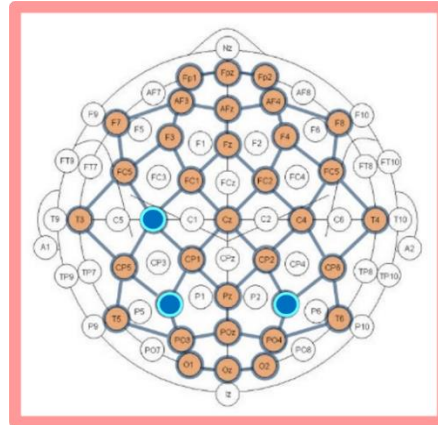


Fig. 7. Positions of EEG acquisition channels selected by the typical testors method

TABLE I
HYPERPARAMETER

Parameter	Value
Epochs	800
Activation function	Softmax
Optimizer	Adam
Batch size	7
Test size	0.3

TABLE II
INFORMATIONAL WEIGHT OF THE ACQUISITION CHANNELS OF EEG SIGNALS FOR THE CLASSIFICATION OF TWO CLASSES OF MI

Channel	Position	Informational weight
C1	FP1	0%
C2	FP2	0%
C3	C3	100%
C4	C4	0%
C5	CP5	0%
C6	CP8	0%
C7	P3	100%
C8	P4	100%

for validation, that is, the algorithm did not know these data during training. Table 1 shows the hyperparameters used for training.

IV. RESULTS

Table 2 shows the informational weight of the acquisition channels of the EEG signals acquired with mental tasks of imagining opening and closing the left hand and opening and

closing the right hand. The table shows that according to the results obtained by the method of analysis by typical testors, the combination of channels C3, P3 and P4 has an informational weight of 100%, which means that the information from sensors C3, C7, C8 is relevant to distinguish between the two mental tasks.

Figure 7 shows in the blue areas of the location of the acquisition channels selected by the typical testors, as mentioned above, the channels are C3, P3 and P4.

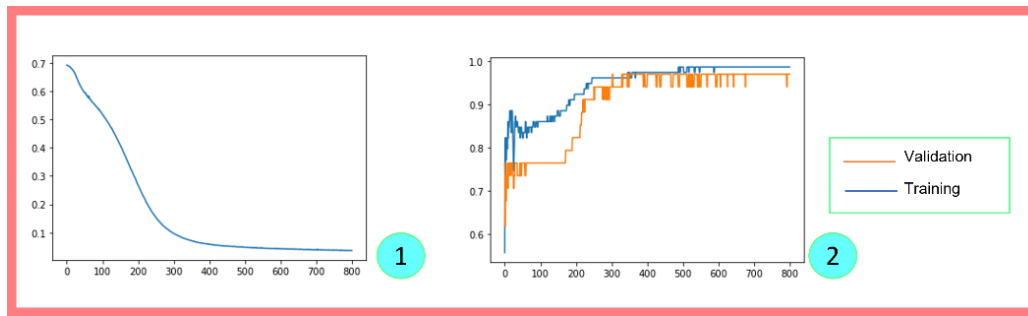


Fig. 8. Training and validation plots. 1: Loss graph. 2: Accuracy graph showing training and validation

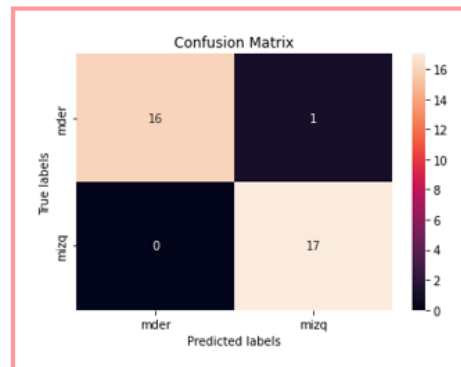


Fig. 9. Confusion matrix of the classification of EEG signals with MI

The FFT variance feature information was classified using only the information from the channels containing the informational weight of 100%, that is C3, C7, and C8. The training can be observed in the graphs in figure 8, graph 1 shows how the losses were decreasing until reaching 0.1. In addition, graph 2 shows the training graph compared to the validation graph, both graphs are similar, however, the validation graph is more irregular, from epoch 400 it oscillated between 0.94 and 0.97%, the latter being the maximum accuracy reached, while in the validation it reached 98%.

Figure 9 shows the confusion matrix obtained during validation, we can observe that the right-hand MI 16 signals were effectively classified, confusing only one with the left-hand MI. On the other hand, 100% of the left-hand MI signals were correctly classified. Furthermore, in Table 2 we observe the accuracy parameters of the LSTM neural network, which is 97% overall, 94% for the right-hand MI, and 100% for the left-hand MI class. We also obtained a precision of 0.97, which shows us the dispersion of the data, the sensitivity of 1, and the specificity of 0.94, the latter indicating how capable the algorithm is of distinguishing between positive and negative cases.

V. CONCLUSIONS

The analysis of typical testors resulted in the selection of channels C3, C7, C8. On the one hand, the C3 channel belongs to the left-brain area, which is not a coincidence that it is the dominant side of right-handed people, as is the case of the study subject. According to the position of the international electrode placement system 10-20, the brain regions related to the C3 acquisition channel belong to the central part between the frontal lobe, and the parietal lobe corresponds to the primary

motor cortex, which is responsible for modulating the voluntary movement of the limbs.

The acquisition channels located at positions P4 and P5 are part of the parietal lobe, which is located in the primary somatosensory area, this area receives information from the senses but is also responsible for motor coordination. Both brain regions are related to the imagination, sensitivity, and motor skills of the subject.

The LSTM recurrent neural network, on the other hand, has been shown to have the ability to classify electroencephalographic signals using only one feature of the signal by means of a reduced number of neurons and layers.

With the analysis of typical testors, the dimension of the data was reduced by eliminating the irrelevant information for the differentiation of both classes, which went from [8,120,200] to [1,3,120] with this reduction the classification time was reduced.

For the analysis of the results, all 8 acquisition channels were classified under the same conditions mentioned in the experiment. The result was an accuracy of 88%, so our method improved the classification by 9%, this was achieved by eliminating the channels whose characteristics are redundant.

Therefore, it can be concluded from these results for the test subject of this study it is necessary to use the acquisition channels C3, P4, and P5 together to achieve a distinction between the mental tasks of motor imagination of opening and closing the right hand and motor imagination of opening and closing the left hand. This experiment is replicable since the objective was achieved. However, as part of future work, brain signals from a larger number of people will be analyzed and the number of mental tasks with motor imagination will be increased.

REFERENCES

- [1]. A. Singh, A. A. Hussain, S. Lal, H. W. Guesgen, "A comprehensive review on critical issues and possible solutions of motor imagery-based electroencephalography brain-computer interface," *Sensors*, vol. 21, no. 6, pp. 2173, 2021. DOI:10.3390/s21062173.
- [2]. X. Gu, Z. Cao, A. Jolfaei, P. Xu, D. Wu, T. P. Jung and C. T. Lin, "EEG-based brain-computer interfaces (BCIs): A survey of recent studies on signal sensing technologies and computational intelligence approaches and their applications," *IEEE/ACM transactions on computational biology and bioinformatics*, vol. 18, no. 5, pp. 1645–1666, 2021, DOI:10.1109/TCBB.2021.3052811.
- [3]. H. Altaheri, G. Muhammad, M. Alsulaiman, S. U. Amin, G. A. Altuwajri, W. Abdul and M. Faisal, "Deep learning techniques for classification of electroencephalogram (EEG) motor imagery (MI) signals: A review," *Neural Computing and Applications*, no. 35, pp. 14681–14722, 2021. DOI:10.1007/s00521-021-06352-5.
- [4]. C. Ieracitano, N. Mammone, A. Hussain and F. C. Morabito, "A novel explainable machine learning approach for EEG-based brain-computer interface systems," *Neural Computing and Applications*, vol. 34, pp. 11347–11360, 2021. DOI:10.1007/s00521-020-05624-w.
- [5]. X. Deng, B. Zhang, N. Yu, K. Liu and K. Sun, "Advanced TSGL-EEGNet for motor imagery EEG-based brain-computer interfaces," *IEEE Access*, vol. 9, pp. 25118–25130, 2021. DOI:10.1109/ACCESS.2021.3056088.
- [6]. M. Z. Baig, N. Aslam and H. P. Shum, "Filtering techniques for channel selection in motor imagery EEG applications: A survey," *Artificial Intelligence Review*, vol. 53, no. 2, pp. 1207–1232, 2020. DOI:10.1007/s10462-019-09694-8.
- [7]. P. Gaur, K. McCreddie, R. B. Pachori, H. Wang and G. Prasad, "An automatic subject specific channel selection method for enhancing motor imagery classification in EEG-BCI using correlation," *Biomedical Signal Processing and Control*, vol. 68, no. 102574, 2021. DOI:10.1016/j.bspc.2021.102574.
- [8]. Y. Liu, Z. Wang, S. Huang, W. Wang and D. Ming, "EEG characteristic investigation of the sixth-finger motor imagery and optimal channel selection for classification," *Journal of Neural Engineering*, vol. 19, no. 1, 2022. DOI:10.1088/1741-2552/ac49a6.
- [9]. Z. A. A. Alyasseri, A. T. Khader, M. A. Al-Betar and O. A. Alomari, "Person identification using EEG channel selection with hybrid flower pollination algorithm," *Pattern Recognition*, vol. 105, no. 107393, 2020. DOI:10.1016/j.patcog.2020.107393.
- [10]. H. R. Hussien, E. S. M. El-Kenawy and A. I. El-Desouky, "EEG channel selection using a modified grey wolf optimizer," *European Journal of Electrical Engineering and Computer Science*, vol. 5, no. 1, pp. 17–24, 2021. DOI:10.24018/ejece.2021.5.1.265.
- [11]. Y. Park and W. Chung, "Optimal channel selection using correlation coefficient for CSP based EEG classification," *IEEE Access*, vol. 8, pp. 111514–111521, 2020. DOI:10.1109/ACCESS.2020.3003056.
- [12]. H. Zhang, X. Zhao, Z. Wu, B. Sun and T. Li, "Motor imagery recognition with automatic EEG channel selection and deep learning," *Journal of Neural Engineering*, vol. 18, no. 1, pp. 01600, 2021. DOI:10.1088/1741-2552/abca16.
- [13]. J. Jin, C. Liu, I. Daly, Y. Miao, S. Li, X. Wang and A. Cichocki, "Bispectrum-based channel selection for motor imagery-based brain-computer interfacing," *IEEE Transactions on Neural Systems and Rehabilitation Engineering*, vol. 28, no. 10, pp. 2153–2163, 2020. DOI:10.1109/TNSRE.2020.3020975.
- [14]. H. Varsehi and S. M. P. Firoozabadi, "An EEG channel selection method for motor imagery-based brain-computer interface and neurofeedback using Granger causality," *Neural Networks*, vol. 133, pp. 193–206, 2021. DOI:10.1016/j.neunet.2020.11.002.
- [15]. D. Gurve, D. Delisle-Rodriguez, M. Romero-Laiseca, V. Cardoso, F. Loterio, T. Bastos and S. Krishnan, "Subject-specific EEG channel selection using non-negative matrix factorization for lower-limb motor imagery recognition," *Journal of Neural Engineering*, vol. 17, no. 2, pp. 026029, 2020. DOI:10.1088/1741-2552/ab4dba.
- [16]. M. T. Soto, A. T. Soto and E. P. de León Sentí, "Algoritmo Genético y Testores Típicos en el Problema de Selección de Subconjuntos de Características, Sistemas, Cibernética e. Informática", vol. 3, no. 2, 2006.
- [17]. E. Alba and R. Santana, "Generación de matrices para evaluar el desempeño de estrategias de búsqueda de testores típicos," *ACI Avances en Ciencias e Ingenierías*, vol. 2, no. 2, 2010. DOI:10.18272/aci.v2i2.23
- [18]. Y. Yu, X. Si, C. Hu and J. Zhang, "A review of recurrent neural networks: LSTM cells and network architectures," *Neural Computing*, vol. 31, no. 7, pp. 1235–1270, 2019. DOI:10.1162/neco_a_01199.
- [19]. <https://openbci.com/>